



The feasibility of using flap gates as constriction flow meters for estimating sanitary sewer overflows (SSO)

Oleksandr Panasiuk*, Annelie Hedström, Richard M. Ashley, Jiri Marsalek, Maria Viklander

Department of Civil, Environmental and Natural Resources Engineering, Luleå University of Technology, 971 87 Luleå, Sweden, Tel. +46 72-539 07 37; email: oleksandr.panasiuk@ltu.se (O. Panasiuk)

Received 15 October 2018; Accepted 19 February 2019

ABSTRACT

Increased awareness of the negative effects of sanitary sewer overflow (SSO) events on human health and aquatic life led to the development of various control measures, of which implementation is impeded by the lack of information on SSO occurrences, flows and volumes. The collection of such information requires data acquisition systems, which can be costly and are fully utilized just during limited time periods of the year. In search for inexpensive approaches to SSO monitoring, the feasibility of using existing flap gate installations, serving for prevention of back-up flows into sewers, as constriction flow meters was investigated, with promising results. An experimental pilot-scale setup was designed to allow steady water flow through a flap gate built into a partition wall between two chambers. The stabilized water heads in the chambers and the flow rate through the flap gate were measured, for both dry and submerged flap gate conditions, and five flap gate sizes (200, 300, 400, 500 and 600 mm), with relatively heavy covers (6–102 kg). The measured data were used to develop flow rating curves, by non-linear regression, in the form $Q = f(\Delta H)$, where Q is the discharge through the flap gate and ΔH is the pressure differential upstream and downstream of the gate. The regression curves fitted the experimental data with high precision ($R^2 > 0.99$). The use of flow rating curves for estimation of the SSO volume was discussed. This study demonstrated that the water head measurements upstream and downstream of the flap gate can provide a reliable, accurate and inexpensive method for quantification of the SSO discharges and volumes.

Keywords: Flap gates; Sanitary sewer overflows (SSO); SSO volumes

1. Introduction

Any untreated or partially treated discharge of wastewater into the environment that may occur during dry or wet weather [1], is referred to as a sanitary sewer overflow (SSO) [2]. A number of reasons may lead to unintended SSO events: additional volumes of Infiltration and Inflow (I/I) reducing the effective capacity of sanitary sewers; increased population contributing sewage; sewer design flaws; blockages; and, breaks in system operation because of maintenance or pump failures [3]. The untreated wastewater from SSO can be transferred through the

overflow systems into the receiving waters, reducing their quality and causing risks to human health, as reported e.g. by Jagai et al. [4] with respect to increased emergency room visits for gastrointestinal illnesses following SSO events. Additional impacts are caused on aquatic organisms [5], and in terms of environmental impacts, SSO are similar to combined sewer overflows (CSO).

Increased awareness of the negative effects of SSOs has led to the development of various control measures as part of watershed protection programs around the world [1,5,6]. As the first step of these programs, the volumes of discharges of untreated wastewater into receiving waters should be

* Corresponding author.

monitored or at least estimated by modelling. However, the information about the number of SSO events is often unknown due to poor or limited monitoring [6,7].

Only conventional flow monitoring at overflow locations can provide information on occurrence, duration and volume of SSO. However, direct flow rate measurements in sewers near the overflow structure location are challenging, and require installation and regular maintenance of relatively expensive equipment [8]. Furthermore, such expensive equipment may be needed and used just few days per year, when SSO occur. Alternatively, there are surrogate methods that can be used for the monitoring of the SSO events: motion, moisture, temperature and water quality sensors; video image analysis; sampling of human specific contaminants like caffeine in the receiving waters; electrical contacts closing during SSO events; as well as various modelling approaches [9–13]. These methods have drawbacks of potential false detections (motion, moisture, temperature, electrical sensors), moderate to high investment, running and maintenance costs (water quality sensors, video image analysis, caffeine sampling), or the lack of long-term monitoring data and a calibrated model for the modelling approaches [10,12].

A further problem is that backflows can occur through an overflow system, when receiving water levels increase and water may back-flow into the wastewater network, as experienced in many locations [14]. This additional relatively clean water often increases the volumes of water that need to be transported to the treatment facility and dilutes wastewater pollutants, resulting in lower treatment efficiency, higher costs for chemicals, and increased electricity consumption for wastewater pumping [15].

Flap gates have been used for a long time for preventing backflows of the receiving waters into the sewer systems [14,16] and their studies focused mostly on reliable operation of flap gates and the head losses caused in the upstream pipe system (Burrows and Edmonds, 1988). Furthermore, many texts on sanitary engineering used the 1936 data produced by the Hydraulic Laboratory of the State University of Iowa for specific “lightweight” gates [14] and, for that reason, found to be of limited value by [17]. Only one reference was found in which it was attempted to estimate flow rates based on the opening angle of the flap gate [6]. However, while the analysis provided general fit of the data, the flow estimates differed from observations in the order of 20%–30%. Furthermore, the study did not report the associated head losses and that limited the usefulness of the reported data for practice [14].

The combination of two abovementioned aspects—the lack of reliable, inexpensive methods for SSO monitoring and the availability of the flap gates for backflows prevention—led to the objective of this paper: use of flap gates as constriction flow meters for the estimation of SSO discharges. In practical terms, this idea requires to establish flow rating curves of flap gates as a function of the water head differential upstream and downstream of the flap gates, with focus on rugged flap gates, with relatively heavy covers, suitable for the sewer environment.

2. Material and methods

2.1. Experimental setup

The experiments were done at the Uddebo wastewater treatment plant in Luleå, Sweden. The experimental setup

consisted of two chambers A and B, with the dimensions of $6.0 \times 6.2 \times 3.75$ m and $5.7 \times 6.2 \times 3.75$ m, respectively (see Fig. 1). The ABS AFP-3003 pump installed in the adjacent room was used to pump water from Chamber B to Chamber A, with the maximum flow rate of about 400 L s^{-1} , through the 300 mm diameter steel pipe. The wall that separated the two chambers was 300 mm thick and had a round opening with the diameter of 800 mm allowing water to circulate from Chamber A back to Chamber B. Around this opening a 950×950 mm U-shaped mounting frame was installed inside Chamber B. Each of the tested flap gates was attached to the 900×900 mm base plate—10 mm thick steel and 5 mm thick rubber sheets glued together—that had an opening of the same diameter as the opening diameter of the attached flap gate. The bolts on the mounting frame pressing the base plate to the wall as well as the silicone sealant applied along the perimeter of the rubber sheet before installation facilitated quick replacement and watertight installation of the tested flap gates.

The location of the intake and the outlet of the metal pipe, the dimensions of the chambers and the position of the opening in the wall between the chambers were fixed and could not be modified; therefore, the effects of the flow conditions in the upstream and the downstream chambers were not studied in the presented paper.

2.2. Flap gates

Five KWT flap gates type KRK-R-F with the opening diameter of 200, 300, 400, 500 and 600 mm were tested (Fig. 2). All had a valve cover angle of 15° (Fig. 2(c)) and relatively heavy covers (6–102 kg). More details of the flap gates used are in Table 1.

2.3. Measurements of pressures

At the bottom of each chamber, a water level meter was installed. The water level meters had an accuracy of $\pm 0.1\%$ of full scale (0–10 m) and were calibrated prior to the experiments using a graduated scale. The flow rate was measured using a KROHNE Waterflux 3000 electromagnetic flow meter mounted in the pressurized 300 mm pipe from

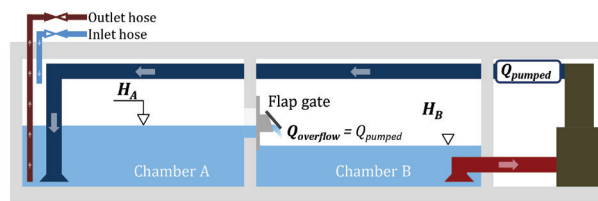


Fig. 1. Experimental setup.

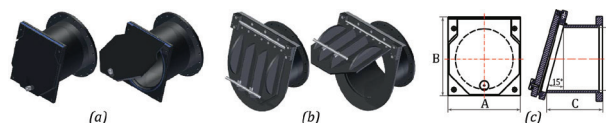


Fig. 2. Appearance of flap gates with the diameter of (a) 200–500 mm and (b) 600 mm; (c) scheme of flap gates dimensions (see Table 1 for more details).

the pump with a KROHNE IFC 100 signal converter with an accuracy of $\pm 0.3\%$ of the measured value. Online signals from the flow meter and the two water level meters were logged at 1 s intervals using an Intab PC-logger 31000-usb.

Water from the nearby Bay of Gräsäl (part of the Gulf of Bothnia) was used in the experiments.

2.4. Description of experimental runs

Experimental runs were performed for each of the flap gates in two setups: submerged and dry (free discharge, see Fig. 3). For the submerged setup, the water head in Chamber B (H_B) was sufficient to keep the flap gate fully under the water; while for the dry setup, H_B was below the flap gate bottom, letting the water pass through the flap gate and fall freely.

Both the submerged and the dry experimental runs were conducted as following: In the initial phase, the water was pumped from Chamber B to Chamber A at a constant flow rate. The water head in Chamber A (H_A) increased and so did the flow through the flap gate. After some time (from 30 s for $\varnothing 600$ mm to 4 min for the $\varnothing 200$ mm flap gate), the heads in both chambers stabilized, indicating that the system had reached an equilibrium state. At this state, the flow

through the flap gate was equal to the measured pump flow. Equilibrium was kept for at least 5 min. Instantaneous flow rates and water heads were measured with 1 s resolution during this period of time, recorded and about 300 values were averaged for each equilibrium state. Then, the pumping flow rate was stepwise increased until the maximum possible flow rate and then stepwise decreased to the minimum possible flow rate and the whole procedure was repeated for each step with the new flow rate. At least 15 repetitions were performed for the submerged set-up and 10 for the dry setup and the new equilibrium values for the flow rate and water heads were obtained as described above. The whole procedure was repeated for the dry and submerged setups for each of the tested flap gates.

2.5. Opening pressure tests

Additional experiments were performed to test the hydrostatic water pressure needed to open the flap gates in both dry and submerged states. The flap gate was defined as open if the bottom of the valve cover moved for at least 5 mm from its closed position. The measurements of this distance were made using a magnetic sensor with an LED indicator that switched off if the cover opened more than 5 mm.

During both dry and submerged experiments serving to evaluate the opening pressure, the head in Chamber A was slowly increased using the inlet water hose (see Fig. 1). As soon as the valve cover opened (LED indicator turned off), the heads in both chambers were recorded. Then some water was pumped out from Chamber A using an outlet hose (see Fig. 1), so the flap gate closed again. The procedure with filling up and pumping out was repeated at least three times and the corresponding heads were measured. For the submerged setup, the opening pressure was determined as the differential head between Chambers A and B water heads ($\Delta H_{subm} = H_A - H_B$). For the dry setup, the opening pressure was calculated as the difference between the head in Chamber A and the flap gate invert level ($\Delta H_{dry} = H_A - H_0$).

Table 1
Flap gates dimensions and opening pressure (see Fig. 2(c) for the dimension scheme) specified by the manufacturer (KWT International)

| D (mm) | A (mm) | B (mm) | C (mm) | Weight (kg) | Opening pressure (mm) | |
|--------|--------|--------|--------|-------------|-----------------------|-----------|
| | | | | | dry | Submerged |
| 200 | 280 | 310 | 265 | 6 | 40 | 20 |
| 300 | 395 | 425 | 265 | 11 | 55 | 30 |
| 400 | 480 | 510 | 315 | 18 | 60 | 30 |
| 500 | 580 | 610 | 315 | 22 | 100 | 39 |
| 600 | 900 | 950 | 465 | 102 | 140 | 57 |

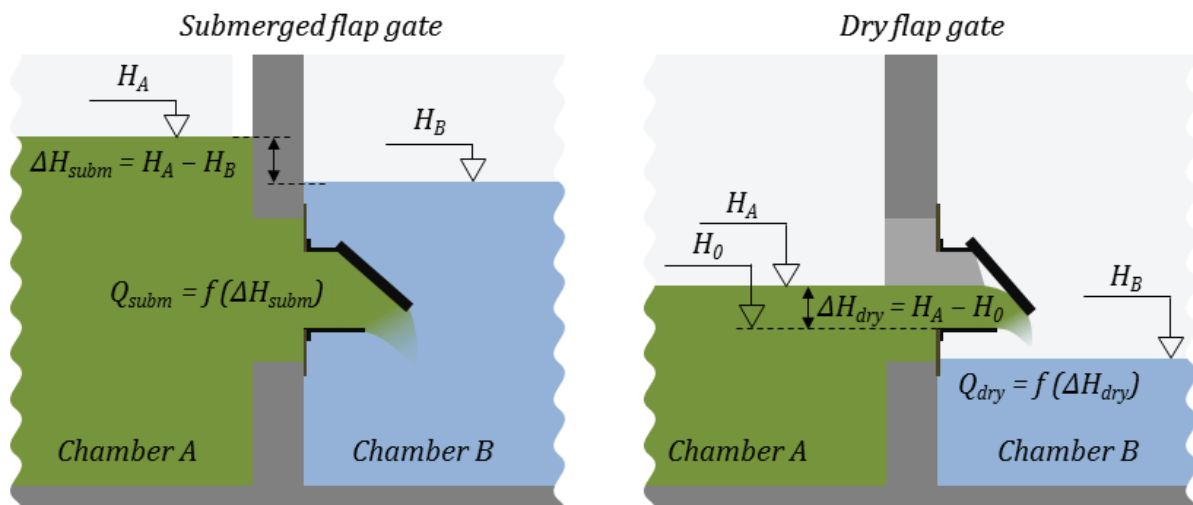


Fig. 3. Scheme of submerged and dry flap gate conditions.

2.6. Backflow prevention tests

Testing of the flap gate performance in prevention of the water backflow was also performed, by raising the head in Chamber B above the flap gate by 0.5 m, while the head in Chamber A was below the flap gate invert. Both heads were measured for at least 14 h.

2.7. Data evaluation

Data retrieval of water heads and flow rate measurements from the logger was performed using Intab EasyView software and then exported to Microsoft Excel. All further data analysis was performed in Microsoft Excel and Minitab Statistical Software. Regression lines were obtained using nonlinear regression method based on Gauss-Newton algorithm in Minitab Statistical Software.

2.8. Development of flap gate rating curves

Replogle and Wahlin [14] analyzed flows through flap gates and concluded that in view of complicated hydraulics, finding a theoretical solution was not feasible. Flap gates open relatively easily, by the hydrostatic pressure exerted by water on the upstream side. However, when the flow is established, the gate is supported by the flow passing through and the gate opening position (angle) depends on both the flow rate and the weight of the gate. The operation of the flap gate is comparable to that of an orifice, whose discharge, Q , is a function of the orifice area (A) and the differential head (h), $Q = C \cdot A (2gh)^{0.5}$, where C is the constant. Thus, flow increases as both A and h increase, with A exerting a larger influence [14]. Regardless of the complexities, the flap gate rating curves can be derived from the measured data by nonlinear regression, which provided the best fit in the following form:

$$Q = \alpha(\Delta H - \beta)^\theta \tag{1}$$

where α and β are fitted constants, θ was assumed to be equal to the theoretical value of 0.5, and ΔH is the differential head. Both constants α and β varied for individual flap gate sizes and the second term in the bracket (β) was positive only in the case of the smallest gate ($D = 200$ mm) and submerged conditions.

3. Results

3.1. Flow rate curves

Based on the results obtained from the experimental runs, the flow rate curves were established for dry and submerged flap gate discharge conditions and each of the various flap gate sizes (Figs. 4, 5 and 6). The goodness of fit of the experimental data to the regression lines that describe flow rate as a function of water head was better than $R^2 = 0.99$ (except for the fully submerged $\varnothing 400$ flap gate in dry conditions, with $R^2 = 0.982$).

For the submerged conditions (Fig. 4), Eq. (1) was used. The best fit curves with variable exponents θ were also established and showed similar results to the theoretical curves with the fixed exponent of 0.5 shown in Fig. 4.

For the dry setup two filling conditions were obtained on the upstream side: partially filled and fully submerged flap gate (dashed and solid lines, respectively, in Figs. 5 and 6). Partially filled flap gate conditions were defined by the water head in Chamber A varying between the invert and crown of the flap gate opening, i.e. $\Delta H \leq D$. As soon as the water head in Chamber A rose above the soffit of the flap gate opening ($\Delta H > D$), the fully submerged conditions were met.

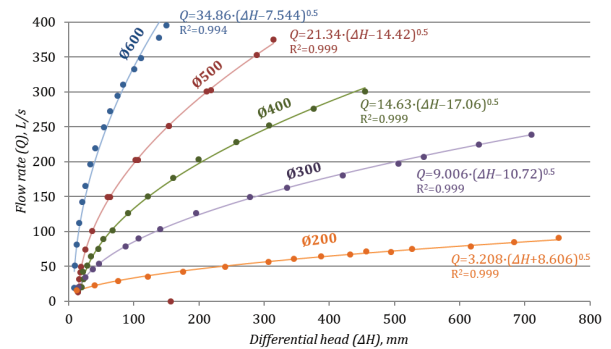


Fig. 4. Flow rate (Q) vs. differential water head (ΔH) curves for various flap gate dimensions (submerged).

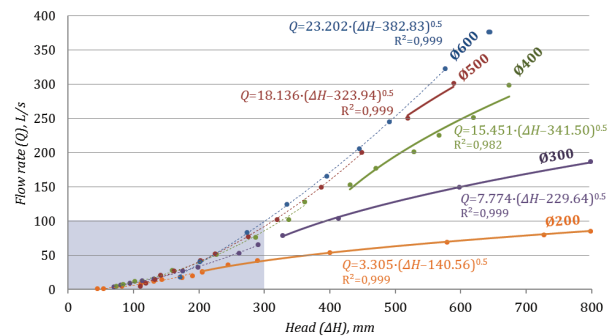


Fig. 5. Flow rate (Q) vs. water head (ΔH) curves for various flap gate dimensions (dry). Dashed lines indicate partially filled flap gate conditions ($\Delta H \leq \text{Diameter}$), solid lines—fully submerged flap gate conditions ($\Delta H > \text{Diameter}$). Highlighted area on the graph is shown magnified in Fig. 6.

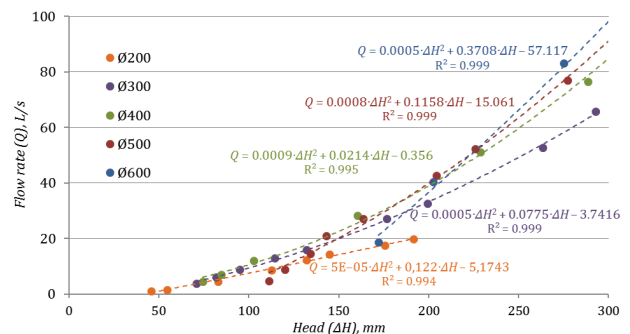


Fig. 6. Flow rate (Q) vs. water head (ΔH) curves for various flap gate dimensions (dry), partially filled flap gate conditions ($\Delta H \leq \text{Diameter}$) (see Fig. 5).

3.2. Opening pressure

The results of the opening pressure tests are presented in Fig. 7. These results were compared with the opening pressure specified by the manufacturer of the flap gates (see Table 1). Additionally, the respective opening pressures were also derived from the flow rate curves (Figs. 4 and 6). In this case, the opening pressure was defined as the differential head at which the flow rate is equal to zero (i.e. where the curve intersects x-axis). The results showed that in all cases (except for Ø200 mm, dry condition) the opening pressures specified by manufacturer were higher than those derived from the flow rate curves and those experimentally obtained (see Fig. 7). This finding is not surprising as the manufacturer most likely used a different definition (more conservative) of the onset of flap gate opening; however, it is important to keep in mind that considerable discharges during SSO events may start earlier and finish later than what the manufacturer’s specifications suggest.

3.3. Flap gates performance in preventing backflows

The results of the backflow leakage testing experiments showed that the maximum backflow rate was observed with the Ø500 mm flap gate: the water head decreased by about 16 mm in Chamber A and increased by about 17 mm in Chamber B, which indicated a backflow rate of about 0.000012 m³ s⁻¹. Such backflow can be considered as negligible.

4. Discussion

4.1. Estimating overflow volumes from the measured differential water head hydrographs of SSO

As the function $Q = f(\Delta H)$ was experimentally obtained in this study, the calculation of the SSO flow rate in practice would only require differential water level measurements, upstream and downstream the flap gate. Integration of this function over the SSO event duration provides the volume of wastewater discharged during the overflow event:

$$\text{SSO volume} = \int_{t_{\text{start}}}^{t_{\text{finish}}} f(\Delta H, t) dt \quad (2)$$

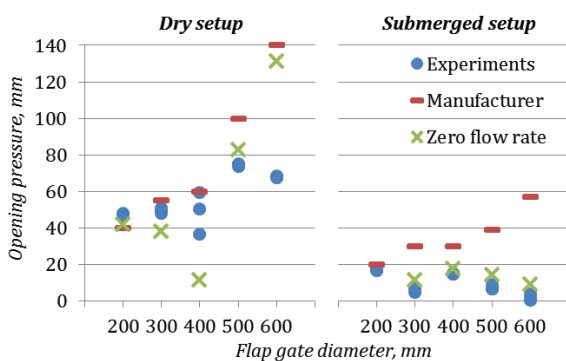


Fig. 7. Opening pressure obtained experimentally, specified by the manufacturer and derived from flow rating curves for dry and submerged setups.

An example of the overflow event for Ø400 mm flap gate in the submerged conditions is presented in Fig. 8. Using the previously obtained function $Q = f(\Delta H)$ for this flap gate, the water head (Fig. 8, the upper panel) can be converted into the flow rate (Fig. 8, the lower panel). The filled area below the function Q line can be integrated between the start and finish times of the overflow event (t_{start} , t_{finish}) and yields the SSO volume. Because of the opening pressure, the duration of the actual overflow event is shorter than the duration of positive water heads, i.e. $t_{\text{finish}} - t_{\text{start}} < t_1 - t_0$. Therefore, Q is set equal to 0 if ΔH is less than the opening pressure ($\Delta H < 18$ mm in this example).

4.2. Accuracy of measured flows

Uncertainties in the empirically derived rating curves originate from two independent sources: uncertainties in the fitted rating curve and uncertainties attributed to water level measurements. In view of the high values of regression coefficients of the fitted data, the first source was neglected (otherwise it could be assessed from residuals of the observed and fitted equation data). The accuracy of the water level meters used in this study was $\pm 0.1\%$ of full scale, which is usually 0–3 m for the pumping stations with the overflow structures, i.e. $\delta h = 3$ mm

As the level of the receiving waters (represented by Chamber B in this study) is relatively stable, the average value ΔH_B could be used for the final calculation of the flow rate. The following formula can be used for the uncertainty for the average value $\delta \Delta H_B$:

$$\overline{\delta \Delta H_B} = \sqrt{\frac{\sum_{i=1}^N \delta h_i^2}{N}} \quad (3)$$

Even half an hour of steady water level measured every second ($N = 1800$) makes uncertainty of ΔH_B negligibly low ($\overline{\delta \Delta H_B} < 0.1$ mm). Therefore, the uncertainties of ΔH both in dry setup ($\delta \Delta H_{\text{dry}} = \delta \Delta H_A$) and in submerged setup ($\delta \Delta H_{\text{subm}} = \sqrt{(\delta \Delta H_A)^2 + (\delta H_B)^2} = \delta \Delta H_A$) were assumed equal

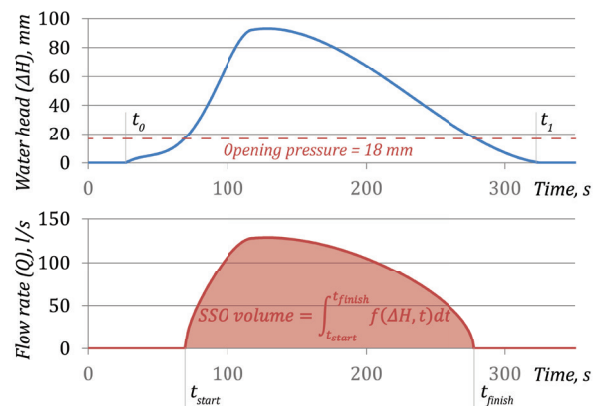


Fig. 8. Example of the overflow event for Ø400 mm flap gate for the submerged conditions. The differential water head changes over the time (above) are converted into flow rates (below), from which the volume of the overflowed water is derived by integration (filled area). Dashed line indicates the opening pressure.

to the uncertainty of a single water head measurement $\delta\Delta H = \delta H = 3$ mm.

The nonlinear regression $Q = \alpha \cdot (\Delta H - \beta)^\theta$ was used for the submerged setup and fully submerged flap gate under dry setup. Consequently, the uncertainty of the flow rate can be calculated as:

$$\delta Q = \left| \frac{\theta \cdot \delta\Delta H}{\Delta H - \beta} \right| \quad (4)$$

The flow rate for the partially covered flap gate in the dry setup was described by the quadratic equation $Q = a \cdot \Delta H^2 + b \cdot \Delta H + c$. The uncertainty of the flow rate function is calculated as:

$$\delta Q = \left| \frac{(2a\Delta H + b) \cdot \delta\Delta H}{Q} \right| \quad (5)$$

Based on Eqs. (4) and (5), the uncertainties of the developed flow rate functions decrease with increased water head ΔH (Fig. 9). In practice, such uncertainties will be below an arbitrary threshold of 5% in 95% of the studied water head range for the submerged setup and in 86% of the range for the partially filled flap gate under dry setup. For the fully submerged flap gate with free discharge setup, the flow rate uncertainties are below 3% for the whole range of monitored water heads.

Beside the uncertainties of the developed flow rate curves discussed above, the accuracy of flow rate estimation depends also on the diameter of the flap gate used. For example, the accuracy of the flow rate measurements for the submerged conditions with $\Delta H = 20 \pm 1$ mm is around ± 0.26 l s⁻¹ for the Ø200 mm flap gate and some ± 5.2 l s⁻¹ for the Ø600 mm flap gate. In order to increase the accuracy of the flow rate measurements, especially with larger diameters of the flap gates, the water level meters used should provide sufficient accuracy (e.g., float-operated shaft encoder and ultrasonic meters that are currently available on the market can have the resolution of around 1 mm).

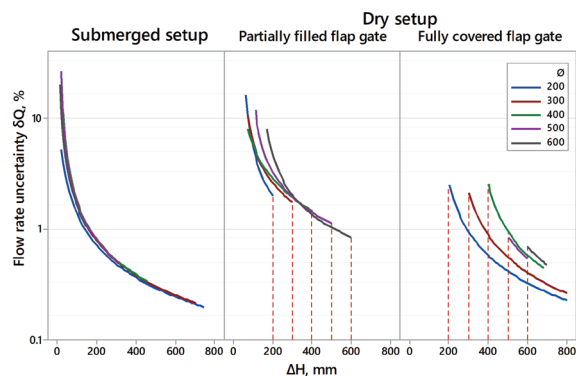


Fig. 9. Uncertainties in the flow rate functions (δQ) vs. water head (ΔH) curves for various flap gate dimensions under submerged setup (left) and dry setup: partially filled (center) and fully covered (right) flap gates. Vertical dashed lines indicate the corresponding flap gate diameter.

Number of factors affect the flow rating curve and the opening pressure of the flap gate: the weight of the cover, its elasticity (in the case of flap gates with a rubber flexure hinge), angle at which the flap gate is attached, geometry of the entrance into the flap gate, flap hinge location, etc. [6,14]. For example, the earlier literature reported lighter, vertically attached flap gates connected to the pipe [e.g., 17]. Such configurations will produce considerably lower head losses to the point, where the flap is supported by the discharging water and head losses barely increase with increasing flow. However, such conditions are more applicable in water level control in irrigation networks rather than in the prevention of sewer backflows studied in this paper.

4.3. Implementation of flap gate flow metering in sewer systems

Water head measurements upstream of the flap gate are already available at most of the pumping stations with overflow systems. Moreover, in some cases the level of the receiving waters is monitored at municipal measuring sites and could be used as the water head downstream of the flap gate. The flow rating curves as obtained in this study could be easily programmed for online measurements as they do not require large-scale computations. If needed, it would be also possible to download logged water head measurements and perform computations of the historical volumes of the overflows.

Finally, the experiments in this study were carried out using clean water from an estuary, whereas real sewers may carry coarse wastewater solids. While the flow rating curves would be still applicable, the wastewater debris may prevent the flap gate from fully closing. This may decrease the performance of the flap gate in preventing the backflow from the receiving waters or decrease the opening pressure of the flap gate causing some undetected wastewater discharges. Rubber-coated flap gates were recommended for minimizing the risks of debris lodging in the flap gate opening [14]. Additionally, the particles in highly turbid receiving waters (e.g., sandy rivers) may settle on the submerged flap gate, increasing its opening pressure [18]. To maintain the proper functioning of flap gates, regular inspections and removal of sediment and debris are recommended.

5. Conclusions

Field experiments with flap gates indicated that it was feasible to use water head measurements, upstream and downstream of the flap gate, in conjunction with flow rating curves, for simple and reliable estimation of the overflow flow rate of SSO or CSO events. The established flow rating curves showed a high precision ($R^2 > 0.99$) for the studied range of flap gate diameters (200, 300, 400, 500 and 600 mm) and examined flow rates (up to around 400 l s⁻¹) for both free discharge (dry) and submerged flow conditions, with covers weighing 6–102 kg.

The results for the opening pressure tests deviated from the manufacturer's data. In most cases, the experimental opening pressure was lower than the specified one, meaning that the overflow events would start earlier and finish later than was expected.

Integrating the flow rating curve over the time can provide a reliable estimation of the volume of an SSO event. The actual opening pressure for the flap gate should be taken into consideration, as the results of this study indicated some deviations from the opening pressure values specified by the manufacturer of the flap gates.

Finally, the water head measurements upstream and downstream of the flap gate can be recommended for use in practice as a reliable, inexpensive and accurate method for the estimation of the flow rates and volumes of overflow events, under similar conditions as described in the paper. Regular inspection and maintenance need to be performed to minimize the risk of gate blockage by coarse solids conveyed by wastewater.

Acknowledgements

This work has been done with the financial support from the Luleå municipality and the Research Council Formas (2012-618), within the Stormwater & Sewers (Dag & Nät) research cluster. This support is gratefully acknowledged. The authors would also like to thank Lars Brännvall and Håkan Tallude as well as the other staff of Uddebo wastewater treatment plant in Luleå for their practical help with the experimental setup.

References

- [1] L. Wright, J. Heaney, S. Dent, C. Mosley, Optimization of Upstream and Downstream Controls for Sanitary Sewer Overflows, in: *Urban Drain. Model.*, American Society of Civil Engineers, 2001: pp. 156–164. Available at: <http://ascelibrary.org/doi/abs/10.1061/40583%28275%2916> (Accessed 30 August 2015).
- [2] J.B. Golden, An introduction to sanitary sewer overflows, in: Office of Water, Washington, D.C., 1996.
- [3] R. Field, T.P. O'Connor, Control strategy for storm-generated sanitary-sewer overflows, *J. Environ. Eng.* 123 (1997) 41–46.
- [4] J.S. Jagai, S. DeFlorio-Barker, C.J. Lin, E.D. Hilborn, T.J. Wade, Sanitary sewer overflows and emergency room visits for gastrointestinal illness: analysis of Massachusetts data, 2006-2007, *Environ. Health Perspect.* 125 (2017) 117007.
- [5] A. Rechenburg, C. Koch, T. Claßen, T. Kistemann, Impact of sewage treatment plants and combined sewer overflow basins on the microbiological quality of surface water, *Water. Sci. Technol.*, 54 (2006) 95–99.
- [6] R. Burrows, G.A. Ockleston, K.H.M. Ali, Flow estimation from flap-gate monitoring, *Water. Environ. J.*, 11 (1997) 346–355.
- [7] P. Kolsky, D. Butler, Performance indicators for urban storm drainage in developing countries, *Urban Water.*, 4 (2002) 137–144.
- [8] A. Campisano, J.C. Ple, D. Muschalla, M. Pleau, P.A. Vanrolleghem, Potential and limitations of modern equipment for real time control of urban wastewater systems, *Urban. Water. J.*, 10 (2013) 300–311.
- [9] G. Gruber, S. Winkler, A. Pressl, Continuous monitoring in sewer networks an approach for quantification of pollution loads from CSOs into surface water bodies, *Water. Sci. Technol.*, 52 (2005) 215–223.
- [10] T. Hofer, A. Montserrat, G. Gruber, V. Gamerith, L. Corominas, D. Muschalla, A robust and accurate surrogate method for monitoring the frequency and duration of combined sewer overflows, *Environ. Monit. Assess.*, 190 (2018) 209.
- [11] G. Leonhardt, S. Fach, C. Engelhard, H. Kinzel, W. Rauch, A software-based sensor for combined sewer overflows, *Water. Sci. Technol.*, 66 (2012) 1475–1482.
- [12] A. Montserrat, O. Gutierrez, M. Poch, L. Corominas, Field validation of a new low-cost method for determining occurrence and duration of combined sewer overflows, *Sci. Total. Environ.*, 463–464 (2013) 904–912.
- [13] O. Wani, A. Scheidegger, J.P. Carbajal, J. Rieckermann, F. Blumensaat, Parameter estimation of hydrologic models using a likelihood function for censored and binary observations, *Water. Res.*, 121 (2017) 290–301.
- [14] J.A. Replogle, B.T. Wahlin, Head loss characteristics of flap gates at the ends of drain pipes, *Trans. Am. Soc. Agric. Eng.*, 46 (2003) 1077–1084.
- [15] R. Wirahadikusumah, D.M. Abraham, T. Iseley, R.K. Prasanth, Assessment technologies for sewer system rehabilitation, *Autom. Constr.*, 7 (1998) 259–270.
- [16] S.B. Mitchell, E. Tinton, H. Burgess, Analysis of flows and water levels near tidal flap gate, *Proc. Inst. Civ. Eng. Marit. Eng.*, 159 (2006) 107–112.
- [17] R. Burrows, J. Emmonds, Energy head implications of the installation of circular flap gates on drainage outfalls, *J. Hydraul. Res.*, 26 (1988) 131–142.
- [18] P. Wu, J. Wang, Effects of sediment pressure on opening of hydraulic automatic control flap gate, *Adv. Sci. Technol. Water. Resour.*, 34 (2014) 79–81.